JOURNAL OF CATALYSIS 130, 498–513 (1991)

Catalytic Reactions of *n*-Alkanes on β-W_2C and WC: The Effect of Surface Oxygen on Reaction Pathways

FABIO H. RIBEIRO, MICHEL BOUDART, RALPH A. DALLA BETTA, AND ENRIQUE IGLESIA*,[1]

*Department of Chemical Engineering, Stanford University, Stanford, California 94305-5025, and *Corporate Research Laboratories, Exxon Research and Engineering Company, Route 22 East, Annandale, New Jersey 08801*

Received November 21, 1990; revised February 26, 1991

Tungsten carbide powders with WC and β-W_2C structures catalyze alkane hydrogenolysis reactions. Alkanes adsorb on fresh carbide surfaces strongly, leading to rapid deactivation by carbon fragments and to high selectivity to hydrogenolysis products. *n*-Hexane isomerization or dehydrocyclization products were not observed on fresh carbides. Chemisorbed oxygen lowers the binding energy of adsorbed intermediates and decreases both hydrogenolysis and deactivation rates. Oxygen-exposed carbides catalyze *n*-hexane and *n*-heptane isomerization with high selectivity (74–99%). Isomerization involves methyl-shift pathways that require alkene intermediates. These results and the well-known acid properties of WO_x surface species suggest that oxygen-exposed tungsten carbides catalyze bifunctional (dehydrogenation/carbenium-ion) alkane isomerization pathways.

1. INTRODUCTION

Emerging needs for isomeric fuels have led to increased emphasis on heterogeneous alkane isomerization and alkylation catalysis. Strong solid acids and bifunctional noble metal catalysts are typically required for this conversion chemistry, but frequently exhibit poor selectivity and stability. Here, we describe high-surface-area tungsten carbides (30–120 $m^2\ g^{-1}$), modified by strongly chemisorbed oxygen species, which catalyze dehydrogenation and methyl-shift isomerization reactions of *n*-alkanes.

Previous reports described the unique effect of chemisorbed oxygen on the catalytic behavior of tungsten carbides (*1*). Fresh carbides catalyze neopentane hydrogenolysis with turnover rates similar to those on Ru, one of the most active metals in hydrogenolysis reactions. Chemisorbed oxygen decreased hydrogenolysis turnover rates by a factor of about 100 and led to the detection of isopentane among reaction products. Isomerization of alkanes and cycloalkanes that can dehydrogenate to alkenes (e.g., 3,3-dimethylpentane, methylcyclohexane) involves methyl-shift reactions of unsaturated intermediates (*1*). These results suggest that oxygen-exposed tungsten carbides contain acid sites capable of catalyzing carbenium-ion rearrangements of alkene and cycloalkene intermediates.

Here, we describe the reaction chemistry of *n*-alkanes, molecules that can convert to alkenes by dehydrogenation, on fresh and oxygen-exposed tungsten carbides. The results of this study confirm and extend our previous findings and conclusions (*1*).

2. METHODS

Synthesis procedures, chemisorption and physisorption measurements, and methods for temperature-programmed reduction (TPR) and catalytic evaluation of carbides were previously described (*1*, *2*). All experiments were performed in a quartz apparatus that allows carbide synthesis and adsorp-

[1] To whom correspondence should be addressed.

0021-9517/91 $3.00

tion, TPR, and catalytic measurements without exposing samples to air.

Two tungsten carbide phases (WC and β-W_2C) were used in this study. They were prepared using WO_3 (99.9994%; Johnson–Mathey, Puratronic Grade) as the starting material [1, 2]. β-W_2C samples were prepared by nitriding WO_3 with NH_3. The resulting β-W_2N was converted to β-W_2C by treating it with a CH_4/H_2 mixture at 700–1150 K. WC samples were prepared by heating in He to 1100 K and exposing them to flowing CH_4/H_2 mixtures at this temperature for 6 h. Polymeric carbon was removed by a hydrogen treatment at 973 K for 0.8 h.

The effect of chemisorbed oxygen on catalytic and chemisorptive properties was examined by exposing fresh carbide samples to O_2 at 300–800 K and then treating them in H_2 at 673 K for 2 h. Fresh carbide samples were exposed to oxygen at RT by leaking O_2 into the cell slowly (0.1 μmol s^{-1} g^{-1}, 0.1–0.3 g sample, 70-cm^3 cell volume) to prevent exotherms and bulk conversion to WO_3. Oxygen uptakes were about one monolayer at RT. These samples were then heated to 573–800 K for about 0.25 h in O_2 (20 kPa) to increase oxygen uptakes (to four to five monolayers) and residual oxygen coverages after H_2 treatment ($\gtrsim$0.5 monolayer). Samples exposed to O_2 are identified by the exposure temperature (e.g., WC/O–700 K). A small fraction (0.5%) of the chemisorbed oxygen reacted with carbidic carbon to give CO_2 and CO during the oxygen treatment; these products were detected by condensing them into a cold trap (77 K), evacuating the O_2, warming the trap, and measuring the residual pressure.

Two Pt/SiO_2 catalysts (Catalyst A: 0.5 wt% Pt, 0.61 dispersion; Catalyst B: 0.78 wt% Pt, 0.80 dispersion) were also studied. The preparation of Catalyst A is described elsewhere (*3*); it was activated by oxygen (573 K, 30 s) and hydrogen (673 K, 2 h) treatments. Catalyst B was prepared by incipient wetness impregnation of SiO_2 (Davison 62, W. R. Grace Co.) with a solution of tetraminnenitrate Pt(II) (Engelhard); it was then dried (373 K, 12 h), calcined (air, 573 K, 0.5 h), and reduced (H_2, 0.1 K s^{-1}, 773 K, 4 h). Pt dispersion was determined by hydrogen titration of chemisorbed oxygen at RT (*7*).

n-Hexane conversion rate and selectivity were measured in a single-pass gradientless flow reactor. Dihydrogen (40 μmol s^{-1}) was saturated with *n*-hexane by contact with the liquid hydrocarbon at 273 K in an evaporator–condenser system. The resulting mixture contained 6 mol% *n*-hexane. *n*-Hexane (Protex, UV Grade, Baker) was purified by contacting it with a mixture of concentrated H_2SO_4 and HNO_3, drying over $CaCl_2$, distilling, and passing it through activated Al_2O_3 (*4*). This procedure removes olefinic and aromatic impurities as well as any heteroatom (N, S, Cl, Br) compounds (*5*). Purified *n*-hexane contained traces of 2-methylpentane (0.1%) and 3-methylpentane (1%); these impurities were subtracted from product analyses in our calculations of reactant conversion rate and selectivity. Hydrocarbon concentrations were measured by gas chromatography (30% DC-200 on 60/80-mesh Chromosorb P-AW, 3m × 3mm, Alltech Associates) using flame ionization detection.

n-Heptane (Fluka, >99%) reactions were studied in a gradientless recirculating quartz reactor (400-cm^3 total volume) (*1, 6*) at 623 K and 4.4-kPa hydrocarbon and 96-kPa dihydrogen pressures on WC/O–800 K and on Pt/SiO_2 (Catalyst B). Products were analyzed by capillary chromatography using flame ionization and mass spectrometric detection (crosslinked methyl-silicone column; Hewlett–Packard 5880 GC, 5993A GC/MS).

Reactant conversion rates are reported here as turnover rates (v), defined as the number of reactant molecules converted per surface site in the catalyst charge (i.e., the number of turnovers) per second. Site densities are determined by chemisorption measurements, as previously described. Product formation rates are reported as site–time yields, defined as the number of reactant

molecules converted to a given product per surface site per second. Turnover rates reflect single-surface sojourn events whereas site–time yields simply reflect the combined effects of primary and secondary reaction events on the measured rate of appearance of individual reaction products. Selectivity is reported either as molar selectivity or as the percentage of converted reactant molecules that appears as a given product (carbon selectivity).

Chemisorption uptakes (CO, H_2, RT) and BET surface areas (N_2, 77 K) were measured before *n*-hexane catalytic tests using procedures described previously (*1*). Then, *n*-hexane reaction rates and selectivities were measured until they reached steady-state values (~4 h) and the reaction temperature was varied to obtain activation energies. The catalyst was then flushed with H_2 for 0.6 ks at reaction temperature, evacuated (~10^{-8} Pa), and heated to 800 K *in vacuo*; at this point, chemisorption uptakes and BET surface areas were again measured.

3. RESULTS AND DISCUSSION

3.1. Characterization of Fresh Tungsten Carbides

Tungsten carbide powders prepared by carburization of WO_3 (WC) or β-W_2N (β-W_2C) precursors did not chemisorb CO or hydrogen at RT, suggesting extensive contamination by polymeric carbon. The carbon contaminant was removed as methane during a subsequent hydrogen treatment at 973 K for 0.8 h (*1, 2*). Carbon removal increases irreversible CO and hydrogen chemisorption uptakes and BET surface areas and leads to the values reported in Table 1 (*1, 2*). These carbide surfaces are free of excess polymeric carbon and adsorb between 0.2 and 0.4 monolayer of CO and H (2–4 $\times$ 10^{14} cm^{-2} surface density). CO and H surface densities are very similar on a given sample, suggesting that strongly adsorbed forms of both titrants measure tungsten carbide surface sites (*1, 2*); these surface densities are used throughout this study in calculating reaction turnover rates. On both catalysts, CO and H coverages are well below one monolayer. The bulk structure of these carbide materials was established by X-ray diffraction; it corresponds to WC and β-W_2C (*8*). The surface of these carbide samples is not carbon deficient; the detailed surface characterization of these materials is described elsewhere (*1, 2*).

3.2. n-Hexane Hydrogenolysis on Fresh Tungsten Carbides

Initial *n*-hexane hydrogenolysis turnover rates are similar on fresh WC and β-W_2C powders (4×10^{-3} and 6×10^{-3} s^{-1}, at 430 K; Table 1); no isomerization products were detected. Hydrogenolysis activation energies are also similar on the two carbide structures. *n*-Hexane conversion rates decreased with time at all reaction temperatures (Fig. 1, Table 1).

Steady-state turnover rates were calculated using conversion rates after 70–120 turnovers and surface site densities were measured after reaction by hydrogen chemisorption; they were about 20 times lower than initial turnover rates (Table 1).

The specific surface area was unaffected by *n*-hexane reactions but the site density for irreversible hydrogen chemisorption was slightly lower after reaction on both WC (2.3 vs 4.0 $\times$ 10^{14} cm^{-2}) and β-W_2C (1.6 vs 2.0 $\times$ 10^{14} cm^{-2}), suggesting that active sites are blocked by carbonaceous deposits during catalysis (Table 1). These carbonaceous deposits strongly inhibit hydrogenolysis turnover rates even at low carbon coverages because alkane hydrogenolysis is a structure-sensitive reaction; it proceeds preferentially on surface sites that bind reaction intermediates strongly (*1, 9, 10*). Such strong binding sites are selectively deactivated during reaction on nonuniform carbide surfaces. Thus, turnover rates decrease sharply as deactivation proceeds (Fig. 1).

Strong adsorption sites on carbon-deficient carbides can lead to the formation of deposits that selectively destroy the most reactive sites for *n*-hexane hydrogenolysis.

TABLE 1

Physisorption, Chemisorption, and Turnover Rate Data on Fresh Tungsten Carbides[a]

Sample	Initial state			Steady state			E (kJ mol^{-1})
	S_g (m^2 g^{-1})	n_H (10^{14} cm^{-2})	v (10^{-4} s^{-1})	S_g (m^2 g^{-1})	n_H (10^{14} cm^{-2})	v (10^{-4} s^{-1})	
WC	31	4.0	40	32	2.3	2	91
β-W_2C	86	2.0	60	75	1.6	3	97

[a] Conditions: 430 K, 6.1 kPa n-hexane, 94.9 kPa H_2. S_g = specific surface area (from N_2 physisorption at 77 K), n_H = surface number density of irreversibly chemisorbed hydrogen at RT (calculated from hydrogen uptake and S_g), v = turnover rate based on the number of sites measured by irreversible H_2 chemisorption at RT assuming a stoichiometry of one hydrogen atom per site, E = apparent activation energy.

Thus, we also measured turnover and deactivation rates on fresh WC samples pretreated in He (after removal of excess carbon) at 1100 K for 0.5 h (WC–He) or in a mixture of 21 mol% CH_4 in H_2 at 1000 K for 0.5 h (WC–CH_4/H_2). These procedures replenish surface carbon by diffusion from the bulk or by deposition from the carburizing mixture; thus, they titrate any carbon-deficient carbide surface sites before reaction.

Deactivation rates were unaffected by these carburization treatments; they were similar to those measured on fresh carbides (Table 2). Both treatments decreased specific surface areas slightly. Carburization in CH_4/H_2 at 1000 K, without subsequent removal of excess carbon by H_2 at 973 K, leads to significant blockage of chemisorption sites (n_H = 1.2×10^{14} cm^{-2} vs 4.0×10^{14} cm^{-2}) by excess polymeric carbon and to very low turnover rates. The equilibration between surface and bulk phases in fresh samples (He treatment) increases turnover rates slightly but does not inhibit deactivation rates. We conclude that fresh carbide surfaces prepared by our procedure are stoichiometric and in equilibrium with the bulk, as we proposed in previous reports (*2*); therefore, the initial turnover rates and deactivation rates shown in Table 1 are intrinsic properties of stoichiometric tungsten carbide surfaces.

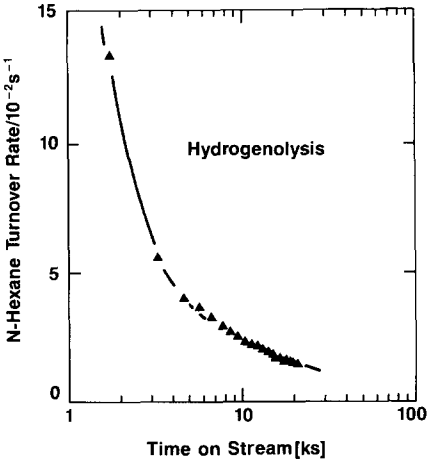

FIG. 1. Site–time yield (STY) versus time plots for n-hexane reactions on WC at 470 K. The sites were counted by irreversible H_2 chemisorption at RT after reaction (6.1 kPa n-hexane, 95 kPa H_2).

Initial hydrogenolysis product distributions on WC and β-W_2C are similar (Table 3). C_1–C_5 n-alkanes were the only products of n-hexane reactions; no isohexanes were detected in the reactor effluent. The extent of multiple hydrogenolysis can be estimated from the average carbon number ($\bar{n}$) of product molecules,

$$\bar{n} = \frac{\sum_{i=1}^{5} i \cdot S_i}{\sum_{i=1}^{5} S_i}, \qquad (1)$$

where S_i is the molar selectivity to hydrocarbons with i carbon atoms. The aver-

TABLE 2

Physisorption, Chemisorption, and Turnover Rate Data on Fresh and Recarburized Tungsten Carbides[a]

Sample	Initial state			Steady state			E (kJ mol^{-1})
	S_g (m^2 g^{-1})	n_H (10^{14} cm^{-2})	v (10^{-4} s^{-1})	S_g (m^2 g^{-1})	n_H (10^{14} cm^{-2})	v (10^{-4} s^{-1})	
WC (fresh)	31	4.0	40	32	2.3	2	91
WC–He	23	4.4	100	17	2.2	3	86
WC–CH_4/H_2	23	1.2	8	22	1.0	0.4	86

[a] Conditions: 430 K, 6.1 kPa n-hexane, 94.9 kPa H_2. S_g = specific surface area (from N_2 physisorption at 77 K), n_H = surface number density of irreversibly chemisorbed H at RT (calculated from hydrogen uptakes and S_g), v = turnover rate based on the number of sites measured by irreversible H_2 chemisorption at RT assuming a stoichiometry of one hydrogen atom per site, E = apparent activation energy.

age number of C–C bonds cleaved per converted n-hexane molecule ($\bar{X}$) is given by

$$\bar{X} = \frac{6 - \bar{n}}{\bar{n}}, \qquad (2)$$

it is near unity on both WC (1.04) and β-W_2C (1.01), suggesting that hydrogenolysis products desorb readily from carbide surfaces before subsequent hydrogenolysis events and that they do not readsorb and undergo secondary hydrogenolysis reactions after desorption. In contrast, neopentane hydrogenolysis on WC leads to multiple C–C fissions (*1*), because strong binding sites that favor extensive dehydrogenation and hydrogenolysis are less severely deactivated by neopentane than by n-hexane. Moreover, the initial adsorbed product of neopentane hydrogenolysis (isobutane) reacts faster than neopentane while the opposite is true in n-hexane hydrogenolysis; hydrogenolysis rates of linear alkanes actually increase with molecular size.

The fraction of single scission hydrogenolysis events that cleave terminal C–C bonds in n-hexane is also similar on WC (0.47) and β-W_2C (0.46) (Table 3). These terminal hydrogenolysis probabilities are

TABLE 3

Initial (I) and Steady-State (s.s.) Product Distributions for n-Hexane Reactions on Tungsten Carbides[a]

Sample		Selectivity (mol% of product)[b]					$\bar{X}$[c]	Terminal hydrogenolysis selectivity[d]	Conversion[e] (%)	Reaction temperature (K)
		C_1	C_2	C_3	n-C_4	n-C_5				
WC	(I)	27	17	15	18	23	1.04	0.47	3.6	428
	(s.s)	28	17	14	16	24	1.08	0.51	1.4	470
β-W_2C	(I)	23	18	18	18	23	1.01	0.46	3.5	425
	(s.s)	28	19	15	17	22	1.08	0.47	2.5	472
WC–CH_4/H_2	(I)	25	17	17	17	24	1.01	0.48	2.3	470
	(s.s)	20	18	18	18	27	0.90	0.50	0.7	519

[a] Conditions: 430 K, 6.1 kPa n-hexane, 94.9 kPa H_2.

[b] C_1 = methane, C_2 = ethane, C_3 = propane, n-C_4 = n-butane, n-C_5 = n-pentane.

[c] Average number of C–C bonds broken per reacted n-hexane molecule [Eqs. (1) and (2)].

[d] Fraction of single-scission hydrogenolysis events that involve terminal C–C bond (statistical value = 0.4 for n-hexane).

[e] (n-C_6 reacted/n-C_6 initial) × 100; n-C_6 = n-hexane.

slightly higher than those expected from random cleavage of C–C bonds in n-hexane (0.40).

Product distributions were unaffected by the presence of carbonaceous deposits that form during n-hexane reactions and that lead to the observed 20-fold decrease in hydrogenolysis turnover rates as the catalyst deactivates (Table 3). Initial and steady-state product distributions, the extent of multiple hydrogenolysis, and the terminal hydrogenolysis selectivity were similar on fresh and deactivated tungsten carbides; the carburized WC sample (WC–CH_4/H_2), with 75% of its chemisorption sites blocked by carbon deposits, also converts n-hexane with similar selectivity. Therefore, hydrogenolysis product distributions appear insensitive to the binding energy of reactive intermediates and to reactive ensemble size, both of which decrease as deactivation proceeds.

We previously reported that chemisorbed oxygen inhibits neopentane hydrogenolysis on WC and β-W_2C and leads to the formation of isopentane, an isomerization reaction product (*1*). We proposed that chemisorbed oxygen introduces new catalytic sites, such as surface WO_x species, that isomerize neopentane via cationic or metallacyclobutane intermediates. Clean carbide surfaces did not catalyze neopentane isomerization. However, we could not rule out that chemisorbed oxygen merely decreased the binding energy of isopentane intermediates, thus allowing their desorption and exit from the reactor before any subsequent hydrogenolysis occurs. Then, because isopentane is much more reactive than neopentane, its concentration would be well below our experimental detection limit.

Our n-hexane results conclusively show that fresh tungsten carbides indeed lack alkane isomerization sites. Methylpentanes were not observed among reaction products; yet hydrogenolysis rates of methyl isomers are not significantly higher than those of n-alkanes on group VIII metals (*11*). Therefore, secondary hydrogenolysis cannot account for their absence among products. We must conclude that isomers are not formed during n-hexane reactions on fresh WC and β-W_2C. Moreover, any carbide sites that bind hydrocarbons strongly and would be selectively titrated by chemisorbed oxygen would also be blocked by carbonaceous deposits formed by strongly interacting n-hexane. Yet, no isomerization products were detected on deactivated (WC, β-W_2C) or on overcarburized (WC–CH_4/H_2) tungsten carbides. We conclude that chemisorbed

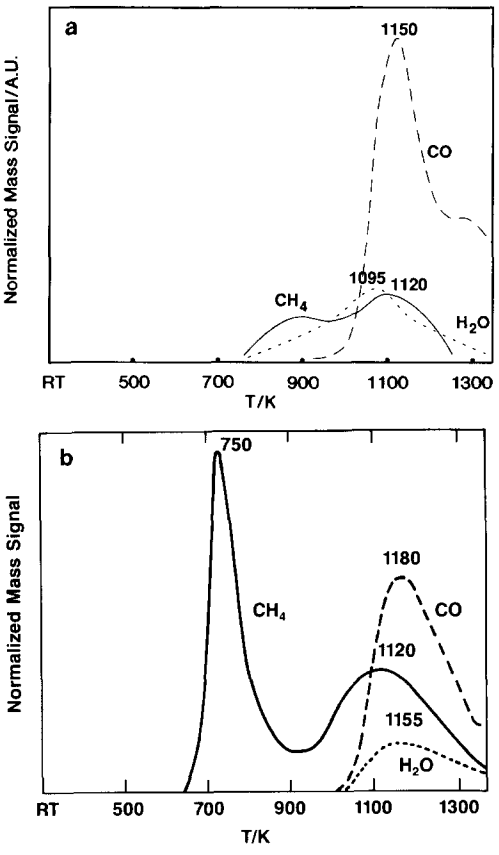

FIG. 2. (a) Temperature-programmed reduction of WC/O–RT in 33% H_2/He after reduction in H_2 at 673 K for 2 h. The amounts of CO, H_2O, and CH_4 were 300, 70, and 80 μmol g^{-1}, respectively. (b) Temperature-programmed reduction (TPR) of WC/O–RT in 33% H_2/He after n-hexane reaction at 630 K. The sample was reduced in H_2 for 2 h at 673 K before reaction. The amounts of CO, H_2O, and CH_4 were 245, 50, and 355 μmol g^{-1}, respectively.

TABLE 4

Specific Surface Area (S_g) and Site Density for Irreversible CO (n_{CO}) and O_2 (n_O) Chemisorption at RT before and after *n*-Hexane Reactions at 630 K on Oxygen-Exposed Tungsten Carbides

Sample	Before reaction		After reaction		
	S_g ($m^2\ g^{-1}$)	n_{CO} ($10^{15}\ cm^{-2}$)	S_g ($m^2\ g^{-1}$)	n_{CO} ($10^{15}\ cm^{-2}$)	n_O ($10^{-15}\ cm^{-2}$)
WC	31	0.39 (0.40[a])	32	0.23[a]	1.39
WC/O–RT	30	0.11	26	0.11	1.0
WC/O–573 K	29	—	24	0.040	1.2
WC/O–700 K	26	—	22	0.091	1.0
β-W_2C	86	0.24 (0.20[a])	75	0.16[a]	1.03
β-W_2C/O–RT	87	0.09	85	0.078	0.7
β-W_2C/O–700 K	65	—	57	0.017	0.5

[a] From hydrogen chemisorption.

oxygen introduces neopentane and *n*-hexane isomerization sites on tungsten carbide surfaces; its role is not to block active hydrogenolysis sites and thus prevent the scavenging of isopentane or isohexane products in secondary hydrogenolysis reactions. Clearly, fresh tungsten carbides lack an isomerization surface function.

3.3. Characterization of Oxygen-Exposed Tungsten Carbides

Fresh carbide samples (after surface cleaning by H_2 at 973 K) were exposed to O_2 at RT (WC/O–RT), 573 K, 700 K, or 800 K, and then reduced in H_2 at 673 K for 2 h. The resulting carbide surface area and site density and the reactivity of chemisorbed oxygen species were determined by adsorption and TPR measurements. The results are shown in Table 4.

The density of CO and hydrogen chemisorption sites is much lower on oxygen-exposed WC and β-W_2C than on the corresponding fresh carbide samples (Table 4). The surface density and reactivity of strongly chemisorbed oxygen (removed by TPR as CO and H_2O above 1000 K) on WC/O–RT before (Fig. 2a) and after *n*-hexane reactions (Fig. 2b) were similar, suggesting that oxygen-exposed carbides maintain chemisorbed oxygen coverages during *n*-hexane reactions. The corresponding oxygen surface density was 0.5–0.7 $\times$ 10^{15} cm^{-2} (~0.5 monolayer). A hydrogen treatment at 673 K for 2 h removes the reactive oxygen that desorbs as water at lower temperature (<700 K) during TPR (Fig. 2a). The strongly chemisorbed oxygen that desorbs as CO above 1000 K is not removed by this hydrogen treatment (673 K) or by reactions of *n*-hexane (630 K) on WC/O–RT.

Larger amounts of residual oxygen were detected after exposure to O_2 at higher temperature. On WC/O–700 K (Fig. 3), for example, residual oxygen coverages were 2.0 $\times$

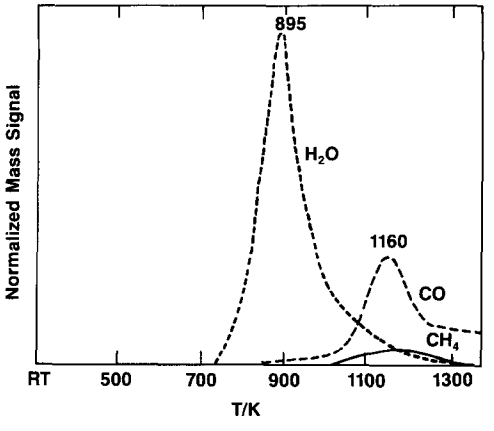

FIG. 3. Temperature-programmed reduction (TPR) of WC/O–700 K in 33% H_2/He after *n*-hexane reaction at 520 K. The sample was reduced in H_2 for 2 h at 673 K before reaction; the amounts of CO, H_2O, and CH_4 were 360, 695, and 35 μmol g^{-1}, respectively.

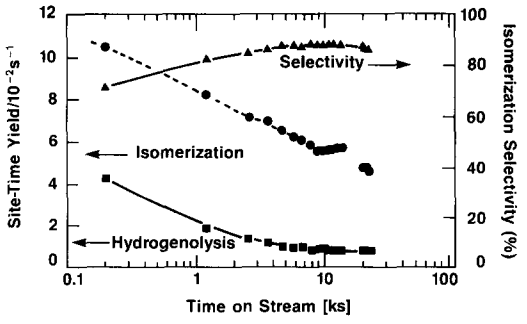

FIG. 4. Site–time yield (STY) versus time plots for n-Hexane Reactions on WC/O–RT at 535 K. The sites were counted by irreversible CO chemisorption after reaction (6.1 kPa n-hexane, 95 kPa H_2; ■, hydrogenolysis site–time yield; ●, isomerization site–time yield; ▲, isomerization selectivity).

10^{15} cm^{-2} (~2 monolayers) after a H_2 treatment at 673 K for 2 h. A large fraction of this chemisorbed oxygen was removed by H_2, predominantly as H_2O, at temperatures (750–950 K) well below those required to remove it, predominantly as CO, from WC/O–RT (>1050 K). The less reactive chemisorbed oxygen species that account for the evolution of CO at high temperature are also present on WC/O–700 K and account for a surface density of 0.75×10^{15} cm^{-2}, a coverage that is slightly higher than that of unreactive oxygen species on carbides exposed to oxygen at lower temperatures (WC/O–RT, 0.5×10^{15} cm^{-2}). Thus, it appears that oxygen titrates strong adsorption sites at all exposure temperatures; more reactive and possibly subsurface oxygen species remain after hydrogen pretreatment at 673 K and during catalytic n-hexane reactions.

The high concentrations of residual oxygen present after 573 and 700 K oxygen exposures (and H_2 treatment at 673 K), however, do not block CO and hydrogen chemisorption sites completely (Table 4), suggesting that much of the excess oxygen lies in subsurface regions or in weakly binding surface sites that do not chemisorb CO or H. Moreover, oxygen chemisorption uptakes on these samples at RT ($1.0–1.2 \times 10^{15}$ cm^{-2} for WC/O–573 K and WC/O–700 K) are very similar to those measured on fresh WC (1.4×10^{15} cm^{-2}) and on WC/O–RT (1.0×10^{15} cm^{-2}, Table 4). This suggests that sites capable of binding oxygen at RT remain on surfaces treated in oxygen and subsequently exposed to H_2 at 673 K. Oxygen-exposed WC powders clearly have submonolayer coverages of chemisorbed oxygen; these coverages increase slightly with increasing oxygen exposure temperature. Yet, much of the higher oxygen content detected at higher exposure temperatures resides below the tungsten carbide surface or in weak binding sites that do not chemisorb CO or hydrogen strongly at RT.

Oxygen chemisorption uptakes at RT are rather insensitive to surface structure (WC or β-W_2C) or to residual oxygen content ($0.07–2.0 \times 10^{15}$ cm^{-2}) and correspond to about one monolayer (Table 4). In contrast, CO and hydrogen surface densities are well below one monolayer and very sensitive to surface structure and to modifications by chemisorbed oxygen. CO uptakes on WC/O–RT are three to four times smaller than on fresh WC and decrease further and markedly as the oxygen treatment temperature increases (Table 4). Clearly, the fraction of total available sites (those titrated by oxygen at RT) that chemisorbs CO decreases markedly in the presence of the additional *surface* oxygen that remains as exposure temperature increases. At higher temperatures, a large fraction of the total oxygen content lies below the reactive carbide surface, but the surface concentration of WO_x species still increases slightly with increasing oxygen treatment temperature.

3.4. *n-Hexane Reactions on Oxygen-Exposed Tungsten Carbides*

Hydrogenolysis and isomerization reactions of n-hexane occur concurrently on oxygen-exposed WC and β-W_2C (Tables 5 and 6). Hydrogenolysis site–time yields on WC/O–RT are about 200 times lower than on fresh WC (Table 5, 520 K). This inhibiting effect of chemisorbed oxygen resembles one reported previously in neopentane hydrogenolysis reactions (*1*). The isomerization selectivity on WC/O–RT was 86% at 520 K

TABLE 5

Steady-State *n*-Hexane Turnover Rates (v_t) and Product Site–Time Yields (STYs) for *n*-Hexane Reactions at 520 K[a]

Sample	STY (10^{-3} s^{-1})[b]			v_t[b] (10^{-3} s^{-1})	r_I[b] (10^{12} cm^{-2} s^{-1})	S_I[b] (%)	x[b] (%)
	H	2-MP	3-MP				
WC[c]	340	0	0	340	0	0	—
WC/O–RT	1.7	7.2	3.2	12	1.1	86	3
WC/O–700 K	0.9	67	35	103	2.05	99	10

[a] Conditions: 520 K, 6.1 kPa *n*-hexane, 94.9 kPa H_2.

[b] Turnover rates and site–time yields are based on the number of sites measured by irreversible CO chemisorption at RT after reaction. H = total rate of hydrogenolysis; 2- and 3-MP = rate of isomerization to 2- and 3-methylpentane; total = total turnover rate of *n*-hexane consumption. r_I = areal isomerization rate; S_I = isomerization selectivity (*n*-C_6 isomers/*n*-C_6 reacted) × 100, *n*-C_6 = *n*-hexane; x = total conversion = (*n*-C_6 reacted/*n*-C_6 initial) × 100.

[c] Rates extrapolated to 520 K from Table 1 data using measured activation energy (91 kJ mol^{-1}).

and increases further (to 99%) as the oxygen treatment temperature increases. The resulting blockage of additional exposed carbide sites leads to a decrease in CO and hydrogen chemisorption uptakes and to a further decrease in hydrogenolysis site–time yields. In contrast, isomerization site–time yields increase by about a factor of 10 and areal rates by a factor of 2 as the oxygen exposure temperature (and the *surface* oxygen coverage) increases from RT to 700 K (Table 5). The twofold increase in areal isomerization rate suggests that higher oxygen exposure temperatures actually increase the density of active WO_x sites. We conclude that chemisorbed oxygen species at carbide surfaces are directly responsible for isomerization reactions, possibly by generating WO_x surface species capable of forming cationic intermediates required in acid-catalyzed isomerization reactions. Indeed, alkane isomerization also occurs with high selectivity on $WO_{2.84}$ (*12*) and WO_x/Al_2O_3 (*13, 14*) catalysts. WC/O–700 K catalysts are very active (v_t = 0.1 s^{-1}) and selective (S_I = 99%) *n*-hexane isomerization catalysts at 520 K (Table 5).

Isomerization selectivity decreases with increasing reaction temperature on all catalysts (Tables 5 and 6); again, it is similar on oxygen-exposed WC and β-W_2C carbides at 630 K. Isomerization site–time yields, areal rates, and selectivity increase markedly with increasing oxygen treatment temperature (Table 6). Hydrogenolysis site–time yields, however, are remarkably independent of exposure temperature (16–25 × 10^{-3} s^{-1}), suggesting that residual active WC_x sites (titrated by chemisorbed CO at RT) are solely responsible for the formation of hydrogenolysis products (Fig. 6).

Hydrogenolysis rates decrease with time on oxygen-exposed tungsten carbides at rates similar to those observed on fresh carbide catalysts (WC/O–RT, Figs. 4 and 5). At 535 K (Fig. 4) and 630 K (Fig. 5), both hydrogenolysis and isomerization site–time yields decrease with time. Deactivation is more severe at 630 K than at 535 K and leads to steady-state *n*-hexane turnover rates that are similar at the two reaction temperatures. At 535 K, isomerization and hydrogenolysis sites deactivate at similar rates, leading to a nearly constant isomerization selectivity (Fig. 4). In contrast, isomerization reactions are selectively inhibited during deactivation at 630 K (Fig. 5). Hydrogenolysis rates on WC/O–RT are less affected and, therefore, isomerization selectivity decreases with increasing time on stream. Deactivation ap-

TABLE 6

Steady-State *n*-Hexane Turnover Rates (v_t) and Site–Time Yields (STYs) for *n*-Hexane Reactions at 630 K[a]

Sample	STY (10^{-3} s^{-1})[b]			v_t[b] (10^{-3} s^{-1}) (total)	r_1[b] (10^{12} cm^{-2} s^{-1})	S_1[b] (%)	x[b] (%)
	H	2-MP	3-MP				
WC/O–RT	16	5.1	2.2	23	0.8	32	7
WC/O–573 K	17	56	320	100	3.5	88	12
WC/O–700 K	25	160	84	280	4.7	89	15
β-W_2C/O–RT	18	3.3	2.6	24	0.46	25	7
β-W_2C/O–700 K	18	83	42	140	2.1	87	5

[a] Conditions: 6.1 kPa *n*-hexane, 94.9 kPa H_2.

[b] Turnover rates and site–time yields are based on the number of sites measured by irreversible CO chemisorption at RT after reaction. H = total rate of hydrogenolysis; 2- and 3-MP = rate of isomerization to 2- and 3-methylpentane; total = total turnover rate of *n*-hexane consumption. r_1 = areal isomerization rate; S_1 = isomerization selectivity = (*n*-C_6 isomers/*n*-C_6 reacted) × 100, *n*-C_6 = *n*-hexane; x = total conversion = (*n*-C_6 reacted/*n*-C_6 initial) × 100.

[c] Rates extrapolated to 520 K from Table 1 data using measured activation energy (91 kJ mol^{-1}).

parently occurs by carbon deposition and not by loss of surface oxygen because a hydrogen treatment at reaction temperature restores initial catalytic rates and selectivity. Also, TPR in H_2/He mixtures before and after *n*-hexane reactions at 630 K showed that no oxygen loss occurs during reaction. After reactions at 630 K, however, a low-temperature CH_4 peak appeared (~700 K, Fig. 2); it was not present after *n*-hexane reactions at 535 K on WC/O–RT, suggesting that carbonaceous deposits form readily during catalysis at these higher temperatures. The CH_4 peak above 900 K arises from removal of carbidic carbon; it occurs on both fresh and used carbide samples.

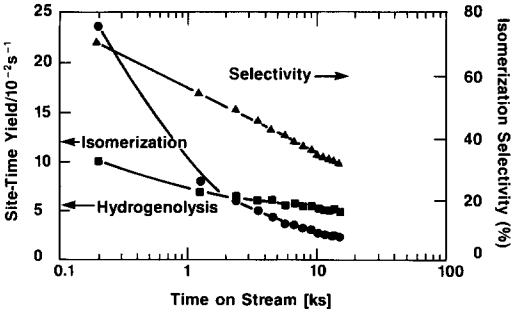

FIG. 5. Site–time yield (STY) versus time plots for *n*-hexane reactions on WC/O–RT at 630 K. The sites were counted by irreversible CO chemisorption after reaction (6.1 kPa *n*-hexane, 95 kPa H_2; ■, hydrogenolysis site–time yield; ●, isomerization site–time yield; ▲, isomerization selectivity).

Steady-state *n*-hexane turnover rates and selectivity on monofunctional (nonacidic) Pt/SiO_2 (Catalyst A) were also measured and compared with those obtained on β-W_2C/O–700 K (Table 7). Turnover rates and selectivities on Pt/SiO_2 were similar to those reported on Pt(111) single crystals (*15*), suggesting that we observe kinetic rates of Pt-catalyzed reactions, unaffected by residual acid sites on the SiO_2 support. Turnover rates on Pt/SiO_2 (0.075 s^{-1}) were somewhat lower than those measured on WC/O–700 K (0.28 s^{-1}) and β-W_2C/O–700 K (0.11 s^{-1}). Isomerization selectivities were also lower on Pt/SiO_2 because of competing (1,5) and (1,6) ring closure reactions (to methylcyclopentane and benzene products, respectively). Ring closure reactions do not occur on WC/O–700 K or β-W_2C/O–700 K at these temperatures (~620 K). The ratio of isomerization rate to hydrogenolysis rate is very similar on Pt/SiO_2 (7.2) and on β-W_2C/O–700 K (6.7).

Alkane isomerization occurs predominantly by hydrogenolysis of C_5-ring intermediates on well-dispersed platinum catalysts

TABLE 7

Steady-State Product Selectivity and Site–Time Yields (STYs) for *n*-Hexane Reactions on β-W_2C/O–700 K and 0.5% Pt/SiO_2 (Catalyst A) (6.1 kPa *n*-hexane, 95 kPa H_2)

Product	Catalyst	
	β-W_2C/O–700 K (T = 614 K)	0.5% Pt/SiO_2, Catalyst A (T = 622 K)
Selectivity (mol%)		
Methane	1.1	1.2
Ethane	3.5	2.5
Propane	6.3	4.9
Isobutane	2.2	—
n-butane	1.7	2.4
Isopentane	1.0	—
n-pentane	0.8	1.8
Dimethylbutane	1.4	—
2-methylpentane	55.2	34.0
3-methylpentane	26.8	13.5
Methylcyclopentane	—	33.1
Benzene	—	6.5
Total *n*-hexane conversion (%)	5.4	6.8
ν_t (10^{-3} s^{-1})[a]	107.0	70
Hydrogenolysis selectivity (%)[b]	13	7.0
Isomerization selectivity (%)[b]	87	50.6
Isomerization/hydrogenolysis ratio	6.7	7.2
Terminal hydrogenolysis selectivity[c]	0.24	0.27
$\bar{X}$ [d]	0.96	1.13

[a] The sites were counted after reaction by irreversible CO chemisorption at RT for the carbide and by H_2–O_2 titration for the Pt sample.
[b] Fraction of converted *n*-hexane appearing as isohexanes (isomerization) or C_1–C_5 products (hydrogenolysis).
[c] Fraction of hydrogenolysis events involving terminal C–C bond (statistical value = 0.4).
[d] Average number of C–C bonds broken per reacted *n*-hexane molecule [Eqs. (1) and (2)].

(*16*). The absence of methylcyclopentane intermediates during *n*-hexane conversion on oxygen-exposed tungsten carbides suggests that isomerization pathways do not involve cyclic intermediates and that, in contrast with Pt, these materials lack a catalytic cyclization functionality.

On Pt, isomerization occurs directly on metal sites; thus isomerization site–time yields provide an accurate measure of site reactivity on Pt. On tungsten carbides, however, isomerization is bifunctional and requires both dehydrogenation and isomerization sites. Site–time yield calculations thus require that we determine the density of those sites (WC_x or WO_x) required for the rate-limiting step in the bifunctional sequence. *n*-Heptane data, discussed in the next section, suggest that alkane dehydrogenation on WC_x sites is a quasi-equilibrated step and that isomerization rates are limited by subsequent WO_x-catalyzed rearrangements of alkene intermediates. Thus, true isomerization site–time yields can be obtained only by measuring the density of WO_x; such measurements are presently unavailable, making turnover rate comparisons with Pt/SiO_2 difficult.

We report areal rates of *n*-hexane isomerization and hydrogenolysis on WC as a function of oxygen treatment temperature and chemisorption site density (n_{CO}) in Fig. 6. The hydrogenolysis areal rate increases linearly with increasing n_{CO}, while that for isomerization actually decreases. It decreases because higher oxygen exposure temperatures increase the density of WO_x species required in the rate-limiting step,

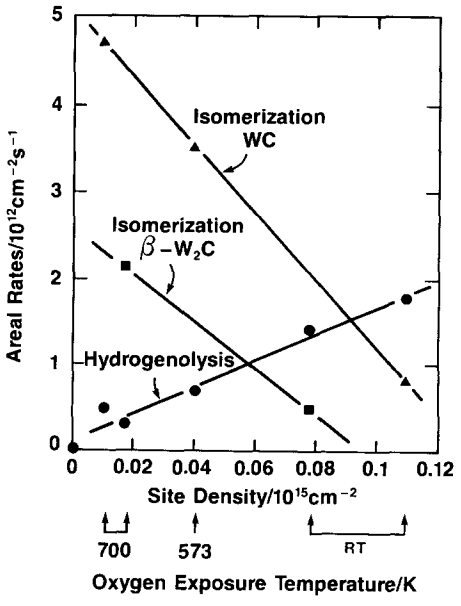

FIG. 6. Areal rates for n-hexane reactions and CO surface densities on oxygen-exposed carbides (630 K, 6.1 kPa n-hexane, 95 kPa H_2).

without decreasing the density of WC_x sites below the number required to maintain alkane dehydrogenation steps at equilibrium. Hydrogenolysis apparently requires only WC_x sites that are accurately counted by strongly adsorbed CO and hydrogen at RT; thus, areal hydrogenolysis increases linearly with increasing WC_x site density.

3.5. *n-Heptane Reactions on WC/O–800 K*

The predicted products of n-hexane isomerization are the same in bond shift and C_5-ring hydrogenolysis schemes. Both mechanisms predict statistical and thermodynamic equilibrium ratios of 2-methylpentane to 3-methylpentane (2 : 1). Indeed, such ratios are typically observed during n-hexane isomerization on oxygen-exposed tungsten carbides. However, n-heptane isomerization product distributions depend on the relative contributions of methyl-shift,

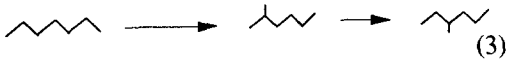

(3)

ethyl-shift,

(4)

and C_5-ring hydrogenolysis pathways (*16*),

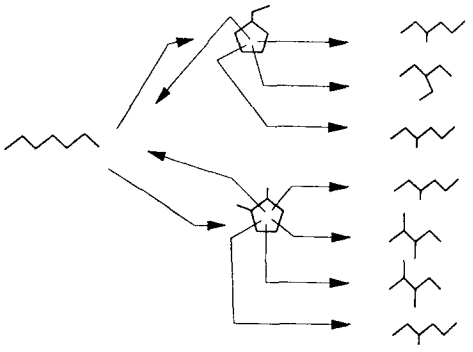

(5)

Methyl-shift isomerization produces predominantly 2-methylhexane as the first product and equal amounts of 2-methylhexane and 3-methylhexane as rapid bond-shift equilibration proceeds; in contrast, C_5-ring hydrogenolysis pathways lead predominantly to 3-methylhexane and 2,3-dimethylpentane products.

Steady-state n-heptane turnover rate (ν_t = 0.117 s^{-1}) and isomerization selectivity (74.3%) on WC/O–800 K (Table 8) are similar to those obtained for n-hexane reactions on WC/O–700 K (0.107 s^{-1}, 87%) (Table 7) and somewhat lower than those for 3,3-dimethylpentane reactions on WC/

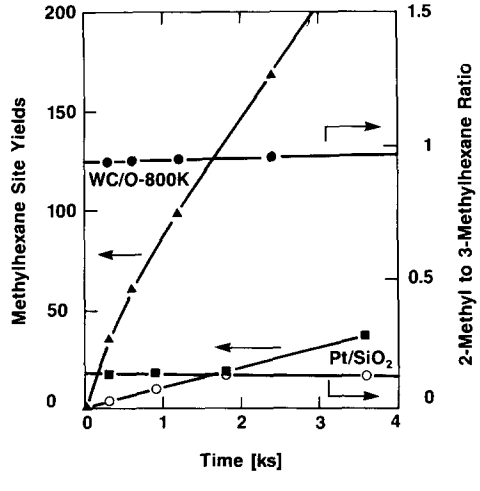

FIG. 7. Isoheptane site yields and 2-methylhexane to 3-methylhexane isomer ratios on WC/O–800 K and Pt/SiO_2 (623 K, 4.4 kPa n-heptane, 96 kPa H_2).

TABLE 8

Steady-State Product Selectivity and Site–Time Yields (STYs) for *n*-Heptane reactions on WC/O–700 K and 0.78% Pt/SiO_2 (Catalyst B) (623 K, 4.4 kPa *n*-heptane, 96 kPa H_2)

	Catalyst	
	WC/O–700 K	0.78% Pt/SiO_2 (Catalyst B)
Carbon selectivity (%)[a]	2.9	0.78
Methane	2.3	1.1
Ethane	2.8	3.2
Propane	0.27	0.65
Isobutane	2.9	3.6
n-Butane	0.37	0
Isopentane	3.8	3.5
n-Pentane	0.8	0.4
Isohexanes	5.2	2.0
n-Hexane	0	1.1
Benzene	33.3	0.75
2-Methylhexane	35.2	6.5
3-Methylhexane	0.1	3.3
2,3-Dimethylpentanes	2.4	0.45
Dimethylpentanes	3.0	2.2
Ethylpentane	0.3	19.2
Ethylcyclopentane	0.2	23.7
1,2-Dimethylcyclopentane	0.5	0.8
Methylcyclohexane	0.37	23.7
Toluene	3.7	3.8
Heptenes		
n-Heptane conversion (%)	8.8	10.5
v_t (10^{-3} s^{-1})	117	134
Hydrogenolysis selectivity (%)[a]	21.8	14.7
Isomerization selectivity (%)[a]	74.3	14.1
Isomerization to hydrogenolysis ratio	3.4	0.96
X[b]	1.21	1.02
Terminal hydrogenolysis selectivity[c]	0.30	0.25

[a] Percentage of converted *n*-heptane appearing as a given product.
[b] Average number of C–C bonds broken per reacted *n*-heptane molecule [Eqs. (1) and (2)].
[c] Fraction of hydrogenolysis events involving terminal C–C bond (statistical value = 0.333).

O–800 K (0.275 s^{-1}, 89%) (*1*). Hydrogenolysis and isomerization are the predominant *n*-heptane reactions; toluene selectivities are only about 0.37% and other cyclization products (alkylcyclopentanes, methylcyclohexane) account for less than 1% of the converted *n*-heptane. Turnover–contact time plots for isoheptane formation in a recirculating batch reactor suggest that 2-methylhexane and 3-methylhexane isomers are produced at similar rates on WC/O–800 K (Fig. 7). Therefore, *n*-heptane isomerization does not occur via C_5-ring hydrogenolysis, because such reaction pathways are unable to form 2-methylhexane isomers as initial products. The 2-methylhexane to 3-methylhexane ratio equals 0.92–0.94 and is independent of contact time (i.e., conversion) (Fig. 7); thus, it reflects primary isomerization events that produce methyl isomers in statistical and thermodynamic distributions. All heptenes (1-heptene, *cis*- and *trans*-2-heptenes and 3-heptenes) quickly reach steady-state concentrations, suggesting their potential role as reactive intermediates in *n*-heptane isomerization. Steady-state heptene to heptane ratios equal their thermodynamic equilibrium values at our reaction conditions (623 K, 96 kPa H_2). Thus, it appears that hydrocarbon dehydrogena-

tion–hydrogenation reactions are fast and do not limit overall reaction rates in the bifunctional dehydrogenation/isomerization sequence.

As in n-hexane reactions, turnover rates for n-heptane reactions on oxygen-exposed tungsten carbides (WC/O–800 K, 0.177 s^{-1}) and Pt/SiO_2 (Catalyst B, 0.134 s^{-1}) are similar (Table 8). On Pt/SiO_2, however, isomerization selectivities (14.1%) are much lower than on WC/O–800 K (74.3%). On Pt/SiO_2 3-methylhexane is the most abundant isoheptane product (Fig. 7), suggesting a significant contribution of C_5-ring hydrogenolysis pathways to the observed isomerization products; 2,3-dimethylpentane is the most abundant dimethylpentane isomer, as expected from C_5-ring hydrogenolysis pathways. The high selectivity to alkylcyclopentanes (42.9%) and toluene (23.7%) products suggests that Pt/SiO_2 catalysts provide cyclization pathways that do not occur on WC/O–800 K. The much lower cyclization and hydrogenolysis rates on WC/O–800 K prevent contributions of C_5-ring hydrogenolysis to n-heptane isomerization pathways.

These results suggest that, in contrast with Pt, oxygen-exposed tungsten carbides isomerize alkanes by methyl-shift rearrangements of alkene intermediates. This proposal is consistent with our previous studies of 3,3-dimethylpentane isomerization on WC/O–800 K (*1*) and with related isotopic tracer studies of competitive n-heptane/heptene reactions (*17*). The initial 3,3-dimethylpentane isomerization products are predominantly 2,3- and 2,4-dimethylpentane, the expected products of methyl-shift reactions, rather than the 2,2-dimethylpentane isomer expected from C_5-ring hydrogenolysis pathways (*1*). Moreover, isomerization apparently proceeds through 3,3-dimethylpentene intermediates. The expected products of 3,3-dimethylpentane isomerization via metallacyclobutane intermediates are not observed. Thus, it is unlikely that metallacyclobutanes contribute significantly to the observed isomer products of n-hexane or n-heptane reactions on oxygen-exposed tungsten carbides.

Bifunctional Reaction Pathways

Oxygen surface adducts actively participate in alkane and alkene isomerization reactions; hydrogenolysis, however, occurs primarily on carbidic surface sites that chemisorb CO and hydrogen strongly at RT. Parallel hydrogenolysis and isomerization pathways are consistent with the selective deactivation of isomerization pathways at 630 K (Fig. 5) and with the observation that hydrogenolysis site–time yields are independent of chemisorbed oxygen coverages while isomerization rates actually increase as oxygen exposure temperature and oxygen coverage increase (Fig. 6).

Our findings can be described by a bifunctional isomerization mechanism that requires alkane dehydrogenation on carbidic surface sites *and* acid-catalyzed methyl-shift reactions of intermediate heptenes on WO_x surface species. Heptenes are in equilibrium with n-heptane during reaction, suggesting that the heptene isomerization step limits the overall bifunctional reaction rate. Thus, the introduction of additional WO_x sites by oxygen exposure at higher temperature, at the expense of strongly binding carbidic sites, increases the overall alkane isomerization rate; in effect, the fewer dehydrogenation sites after oxygen treatment are sufficient to maintain equilibrium alkene concentrations. The presence of acid sites on oxygen-exposed tungsten carbides is consistent with temperature-programmed desorption of preadsorbed NH_3 and with methylcyclohexane isomerization studies on these materials (*1*).

Acid sites can be of Brønsted or Lewis type, depending on whether interacting molecules (bases) acquire a proton (Brønsted) or lose electrons (Lewis) during a surface sojourn. Our measurements do not establish the nature of the surface acidity on oxygen-modified tungsten carbides. Large WO_3 crystallites behave as weak acids (*14, 20*). The acidity arises from abstractable protons

in hydroxyl groups (Brønsted) and from unpaired electrons in W atoms (Lewis) (*20*). Bulk WO_3 contains only octahedral sites; however, WO_x species dispersed on Al_2O_3 at coverages below one monolayer are tetrahedral and introduce strong Brønsted sites onto Al_2O_3 surfaces that normally contain only Lewis sites (*14*). Thus, isolated WO_x species provide Brønsted acid sites; the intermediate role of alkenes in the isomerization catalysis and the nondissociative NH_3 chemisorption that occurs at room temperature suggest that isolated WO_x species on W carbide surfaces, like those on Al_2O_3, lead to Brønsted acid sites.

Similar carbenium-ion mechanisms are likely to contribute to observed isomer products of alkane and alkene reactions on molybdenum and tungsten oxides (*12–14, 18, 19*). Hydrocarbon reactions are likely to partially carburize these metal oxides and thus introduce dehydrogenation sites that permit bifunctional isomerization pathways to occur. In fact, MoO_3/Al_2O_3 (*18*) and WO_3/Al_2O_3 (*13*) have been used in catalytic naphtha reforming; the product distributions are not significantly different from those obtained using modern bifunctional reforming catalysts consisting of Pt or Pt alloys on acidic (halogen-modified) Al_2O_3 supports.

4. CONCLUSIONS

Tungsten carbide surfaces with WC and β-W_2C structures and free of polymeric carbon and residual surface oxygen catalyze *n*-hexane hydrogenolysis with high selectivity; isohexanes are not detected among the reaction products, suggesting that fresh carbides lack an isomerization surface functionality.

Chemisorbed oxygen blocks carbide surface sites that bind CO and hydrogen strongly at RT; oxygen surface coverages increase with increasing O_2 exposure temperature. Chemisorbed oxygen introduces an isomerization functionality onto carbide surfaces. Isomerization site–time yields and areal rates increase markedly as oxygen surface coverage increases, suggesting that WO_x sites are required in rate-limiting steps. Hydrogenolysis areal rates, however, are severely inhibited by titration of carbidic sites with chemisorbed oxygen. *n*-Hexane hydrogenolysis turnover rates (per remaining CO or hydrogen binding site) are independent of oxygen coverage, suggesting that this reaction occurs on remaining strong binding sites present in the carbide surface.

We propose that oxygen surface species participate directly in methyl-shift rearrangements of alkene intermediates. Thus, oxygen-exposed tungsten carbides appear to catalyze both alkane dehydrogenation and carbenium-ion rearrangement reactions characteristic of bifunctional reforming catalysts. They do not, however, catalyze ring closure reactions that typically occur on Pt catalysts.

ACKNOWLEDGMENTS

This work was supported by Department of Energy Grant DE-FG0387ER13762 and by the Exxon Research and Engineering Company. The use of analytical instruments at Catalytica, at the Center for Materials Research at Stanford, and at the Corporate Research Laboratories of Exxon Research and Engineering Company is gratefully acknowledged. We thank Mr. Joseph E. Baumgartner (Exxon) for conducting the *n*-heptane experiments and Dr. Gerhard Raffeis (Stanford) for preparing the WC/O–800 K sample. One of us (F.H.R.) also thanks CNPq of Brazil for a graduate fellowship.

REFERENCES

1. Ribeiro, F. H., Dalla Betta, R. A., Boudart, M., Baumgartner, J. E., and Iglesia, E., *J. Catal.* **129,** in press.
2. Ribeiro, R. H., Guskey, G. J., Dalla Betta, R. A., and Boudart, M., submitted for publication.
3. Schlatter, J. C., and Boudart, M., *J. Catal.* **24,** 482 (1972).
4. Gordon, A. J., and Ford, R. A., *in* "The Chemist's Companion. A Handbook of Practical Data, Techniques, and References," p. 435. Wiley, New York, 1972.
5. Rivera-Latas, F. J., Ph.D. thesis, Stanford University, 1986.
6. Iglesia, E., Baumgartner, J. E., Price, G. L., Rose, K. D., and Robbins, J. L., *J. Catal.* **125,** 95 (1990).

7. Benson, J. E., and Boudart, M., *J. Catal.* **14,** 704 (1965).
8. Powder Diffraction File, "Inorganic Compounds (W. F. McClure, Ed.), JCPDS, Swathmore, 1980; Toth, L. E., "Transition Metal Carbides and Nitrides," Academic Press, New York, 1971.
9. Lee, J. S., Locatelli, S., Oyama, S. T., and Boudart, M., *J. Catal.* **125,** 157 (1990).
10. Sinfelt, J. H., *in* "Advances in Catalysis" (D. D. Eley, H. Pines, and P. B. Weisz, Eds.), Vol. 23, p. 91. Academic Press, New York, 1973.
11. Anderson, J. R., MacDonald, R. I., and Shimoyama, Y., *J. Catal.* **20,** 147 (1971).
12. Ogata, E., Kamiya, Y., and Ohta, N., *J. Catal.* **29,** 296 (1973).
13. Ciapetta, F. G., and Hunter, J. B., *Ind. Eng. Chem.* **45,** 147 (1953).
14. Soled, S. L., McVicker, G. B., Murrell, L. L., Sherman, L. G., Dispenzierre, N. C., Hsu, S. L., and Waldman, D., *J. Catal.* **111,** 286 (1988).
15. Davis, S. M., Zaera, F., and Somorjai, G. A., *J. Catal.* **29,** 296 (1982).
16. Gault, F. G., *in* "Advances in Catalysis" (D. D. Eley, H. Pines, and P. B. Weisz, eds.), Vol. 30, p. 1. Academic Press, New York, 1981.
17. Iglesia, E., Baumgartner, J. E., Ribeiro, F. H., and Boudart, M., *J. Catal.*, accepted for publication.
18. Burch, R., and Mitchell, P. C. H., *J. Less-Common Met.* **54,** 363 (1977).
19. Ciapetta, F. G., Dobres, R. M., and Baker, R. W., *in* "Catalysis" (P. H. Emmett, Ed.), Vol. 6, p. 497. Reinhold, New York, 1958.
20. Ramis, G., Cristiani, C., Elmi, A. S., and Villa, P., *J. Mol. Catal.* **61,** 319 (1990).